IEEE Access
Multidisciplinary | Rapid Review | Open Access Journal

Received 20 February 2024, accepted 16 March 2024, date of publication 21 March 2024, date of current version 27 March 2024.

Digital Object Identifier 10.1109/ACCESS.2024.3380469

RESEARCH ARTICLE

sEMG-Controlled Soft Exo-Glove for Assistive Rehabilitation Therapies

DORIN COPACI[1], (Member, IEEE), DAVID SERRANO DEL CERRO[1], JANETH ARIAS GUADALUPE[1,2], LUIS MORENO LORENTE[1], (Member, IEEE), AND DOLORES BLANCO ROJAS[1]

[1]Robotics Laboratory, Department of Systems Engineering and Automation, Carlos III University of Madrid, Leganés, 28911 Madrid, Spain
[2]Escuela Politécnica Superior, Universidad Francisco de Vitoria, Pozuelo de Alarcón, 28223 Madrid, Spain

Corresponding author: Dorin Copaci (dcopaci@ing.uc3m.es)

This work was supported in part by the National Project Discover2Walk granted by Agencia Estatal de Investigación (AEI) under Grant PID2019-105110RB-C32, in part by STRIDE-UC3M funded by Ministerio de Ciencia, Innovación / Agencia Estatal de Investigación (MCIN/AEI)/10.13039/501100011033 under Grant PDC2022-133898-C32, and in part by the European Union through NextGenerationEU/Plan de Recuperación, Transformación y Resiliencia (PRTR).

ABSTRACT The movement of the human hand offers various degrees of freedom, enabling efficient performance of dynamic tasks and robust interaction with the environment in a compliant and continuous manner. However, the rigid exoskeleton used in hand rehabilitation limits the user's freedom of movement, complicating their natural interaction with the environment. In this study, we present a soft exo-glove for assistive rehabilitation actuated by Shape Memory Alloys (SMA), controlled by a surface electromyography (sEMG) hand gesture classifier. Thanks to the actuator type, the soft exo-glove enables slow, smooth, and controlled movements when activated and provides complete control transparency when the device is not active. This advantage enhances the comfort and acceptance of the exo-glove by the patient. On the other hand, the classifier, in conjunction with the control algorithm and the soft exo-glove, offers the potential to use the exo-glove in assistive hand rehabilitation therapy. For user-friendly use, an interface has been developed, enabling the acquisition of new sEMG data from new users, retraining of the classifier, and connection with the soft exo-glove for rehabilitation therapy. The main objective of this study is to demonstrate that the proposed wearable soft exo-glove, along with the control algorithm and the employed classifier, constitutes an effective solution for assistive rehabilitation tasks, as demonstrated with healthy subjects. Furthermore, this solution can be easily adapted to the users' characteristics and requirements.

INDEX TERMS Assistive rehabilitation, gesture classification, shape memory alloys, soft exo-glove.

I. INTRODUCTION

The human hand is a complex and versatile organ, propelled by an intricate system of muscles and tendons, guided by ligaments and soft tissues, all surrounding a framework of bones. This intricate structure empowers us to perform various daily activities (ADL), ranging from simple tasks like opening a door to manipulating objects, as well as executing more precise movements such as handwriting. The functionality of the hand plays a pivotal role in executing ADL, which are essential for maintaining an independent and healthy quality of life.

According to the World Health Organization, approximately 15 million people worldwide suffer from a stroke each year [1], making it one of the leading causes of disability in adults. Furthermore, about half of these individuals experience hand dysfunction, which impairs their ability to perform ADL effectively. In some cases, this dependence on others for daily tasks becomes a necessity.

Physical rehabilitation is effective for recovering functionality and mobility after a stroke [2]. However, due to its extended duration and the often necessary patient hospitalization, it generates substantial healthcare and social

The associate editor coordinating the review of this manuscript and approving it for publication was Md. Kafiul Islam.

expenses [3]. Therefore, there is a growing interest in exploring new technologies to enhance patients' daily lives and reduce rehabilitation expenses.

In recent years, research on hand exoskeletons has gained significant momentum. Various aspects of this field are under exploration to enhance device hardware, aiming for more compact, soft, effective, and efficient designs. Additionally, efforts are underway to improve cognitive synchronization with users, enabling smoother movements in accordance with user intentions and needs.

In [4], the authors present a rigid hand exoskeleton for both passive and active rehabilitation therapy, utilizing motor impedance. Additionally, Popov et al. [5] introduces a portable glove actuated by motors, designed to assist with ADL. Soft solutions for hand rehabilitation also include glove-based devices. In [6], a soft robotic glove based on pneumatic actuators and controlled by a Brain-Computer Interface (BCI) was tested with 10 patients, with five patients testing only the glove and another five testing the glove controlled by BCI. Although no significant difference was found between the two groups, in the case of the BCI-controlled glove, the authors mentioned a probable trend of prolonged improvements. In [7], a Fishbone-Inspired Soft Robotic Glove with pneumatic actuators for hand rehabilitation, 3D printed, was presented. Due to its structure, this rehabilitation glove permits multiple degrees of freedom (DOF) for each finger. Chen et al. [8] present a pair of soft exo-gloves: one sensorized glove (with flexible and force sensors) for the unaffected hand and an actuated glove powered by micromotors for the affected hand. The authors developed a machine learning algorithm capable of recognizing 6 task-oriented gestures from the unaffected hand using Support Vector Machines (SVM) with an accuracy of 99.07%. This was then replicated with the aid of the actuated glove on the affected limb for task-oriented and mirror rehabilitation therapy. In [9], a soft exo-glove for grasping assistance and rehabilitation driven by sEMG signals was presented. In this study, the grasping force is estimated and then converted into finger displacement.

In this work, we will utilize sEMG signals to detect hand gestures. When our system recognizes the gesture and the user is unable to complete the movement, the exo-glove is activated to complete the hand gesture, as long as the user maintains the intention to complete it. The sEMG signals are an excellent choice for the noninvasive detection of hand gestures. They enable the monitoring of muscle activity and provide valuable information about the intention and movement of the hand without the need for invasive procedures. The EMG signal typically appears about 20-80ms before muscle contraction, allowing for anticipation of motion intention.

The most common classifiers to recognize the hand gestures from sEMG are:

- Support Vector Machines (SVM): SVM is a popular algorithm for classification and is well-suited for tasks involving high-dimensional data [10], [11].
- Convolutional Neural Networks (CNNs): CNNs are highly effective at extracting features from sequential data, such as sEMG signals, and have demonstrated strong performance in gesture recognition [12], [13], [14], [15], [16].
- K-Nearest Neighbors (KNN): KNN is a simple but effective supervised learning algorithm that can be used to classify gestures based on sEMG signals. This algorithm was successfully employed in studies of [17] and [18].
- Recurrent Neural Networks (RNN): RNN is useful for analyzing data sequences, such as sEMG signals, and capturing temporal patterns in gestures. It has been employed in various studies, including [19], [20], and [21].
- Decision Trees: Decision trees are easy to interpret and can be used to classify gestures based on features extracted from sEMG signals, although they are less commonly utilized [22].

Although all algorithms present good accuracy, with the majority achieving more than 90% accuracy in offline databases, the choice of classifier depends on various factors. These factors include the size of the dataset, the complexity of the gestures, and specific performance requirements. The aim of this study is to develop a real-time gesture hand classifier that can generate the necessary reference for the soft exo-glove used in assistive rehabilitation tasks.

In order to carry out assistive rehabilitation therapy for the hand, detecting all sEMG signals can be challenging due to the involvement of many muscles during hand movements. For instance, in the work of Secciani et al. [23], they only placed two skin surface EMG sensors on the forearm, which allows the system to detect three main gestures of the hand: hand opening, hand closing, and relaxed state. In another study [24], prediction of hand grip strength based on sEMG was presented using support vector regression (SVR).

Gesture recognition for controlling the hand exoskeleton in bilateral therapy has been explored in several studies such as [25], [26], and [27].

Other works as [28], are based on sEMG signals to control a hand orthosis have implemented sEMG pattern classification using the Myo Armband. Additionally [29], has used the Myo Armband device to detect five movements of the hand and wrist, including two-finger gripper, wave in, wave out, finger spread, and fist.

In this work, we propose a soft exo-glove device for assistive rehabilitation, controlled according to the sEMG signals. This device is actuated by Shape Memory Alloy (SMA) based actuators, presenting multiple DOFs. Although, the passive rehabilitation exo-glove concept was previously presented in [30], in this work, a new high-level algorithm based in a gesture classifier was developed. This offers the unique capability of individually controlling the extension and flexion of each finger, including thumb opposition, based on the user's intended hand movements detected by the gesture classifier. Among its advantages, the entire

system has been designed to be a compact and comfortable assistive rehabilitation device, it is noiseless during operation, lightweight, user-friendly, and exhibits a low fabrication cost.

This work is divided into four sections. Section II briefly introduces the soft exo-glove design, including its actuators, the EMG acquisition process, segmentation, gesture classification algorithms, the user interface employed in this process, and the proposed high-level control algorithm used for generating real-time references based on identified gestures. Preliminary experimental results are presented in Section III, where the selection of the features, the performance of the classifiers and the first tests with the exo-glove are evaluated. Finally, Section IV and Section V present discussions on the current strengths and limitations of the exo-glove, and the key conclusions drawn from this work.

II. METHODOLOGY

A. SOFT-EXO GLOVE SYSTEM

Our research group has recently focused on the development of exoskeleton devices actuated by SMA. These devices are chosen for their advantageous features, including low weight, noiseless operation, and cost-effectiveness. Their primary purpose is upper limb rehabilitation.

In this work, we employ a soft exo-glove concept previously introduced in a prior study [30]. This soft robotic glove based on neoprene material, is actuated by SMA-based actuators, and it is designed for hand assistance and rehabilitation purposes.

The soft exo-glove, is capable of executing complex movements through individual finger flexion and extension, including opposing motion of the thumb. Each finger is mobilized by two actuators controlled in an antagonist configuration, making it a biomimetic system. The routing of the tendons represents a key element in ensuring the proper functionality of the exo-glove to replicate hand gestures commonly found in ADL, such as gripping.

In Figure 1, key tendon fixation points at the tips of the fingers and the routing of tendons (the three-wire loop) on the proposed soft exo-glove can be observed. When it comes to extension, the most crucial point for tendon routing is at the distal phalanges. If the glove is not perfectly adjusted to the user's hand, there is a risk of bending at the tip of the glove. The configuration we have employed involves the tendons forming a loop over the fingers, effectively preventing the bending of the glove tip. In post-stroke patients, spasticity in the hand is very common and makes it difficult to put on the hand glove. For this reason, the neoprene glove was modified by cutting the material around the middle and proximal phalanges, and relocating the Velcro straps to facilitate the glove placement over the user's hand.

When the fingers are flexed, it is noticeable that the movement of the distal phalanges results in trajectories that are not perfectly parallel. Instead, these trajectories exhibit a slight deviation as they converge towards a common point in the forearm. To ensure a better alignment with the movement of the fingers, this characteristic has been implemented in the soft exo-glove. This can be observed in the fixed tendon routing points on the flexion side of the soft exo-glove, particularly those closest to the forearm.

FIGURE 1. Tendon routing over the soft exo-glove: for the flexion movement - right side and for the extension movement - left side.

The thumb's most critical motion is opposition, characterized by abduction combined with rotation at the carpometacarpal (CMC) joint, which moves the thumb toward the tip of the little finger [31]. This complex movement is achieved in the soft exo-glove through the action of two tendons located on the flexion side. One of these tendons forms a loop over the little finger for thumb opposition, while the other follows a path along the palm before deviating towards the forearm for thumb flexion.

The actuation of the soft exo-glove relies on SMAs as the core technology. In this work, the Joule effect is utilized to generate heat within the SMA fibers. This process involves the conversion of electrical energy into thermal energy, which, in turn, is transformed into mechanical work. During this transformation, as the SMA fibers shift between the martensite and austenite phases, they contract by up to 4% of their original length.

The actuator is connected to the exo-glove tendon system within a sensorized box [30]. This enclosure includes a linear potentiometer (PTA4543-2015CPB103, 12 bits resolution) to measure the actuator displacement, along with a mechanism designed to duplicate the final displacement. The actuator generates a tendon displacement of 80 mm with a force of 17.5 N for each finger.

The electronic hardware comprises position sensors, a microcontroller, and a power circuit necessary for controlling the SMA-based actuators. The power circuit for the SMA wires is built around MOSFET transistors. These transistors are activated through Pulse Width Modulation (PWM) signals generated by the microcontroller. They regulate the flow of power to the actuators as required. With this electronic hardware setup, the control system can effectively manage up to 12 different actuators, with each actuator potentially utilizing one or more SMA wires.

The SMA-based actuator exhibits nonlinearities and significant hysteresis, posing challenges for employing traditional nonlinear control methods to achieve optimal performance. To address these nonlinearities in the exo-glove control, a Bilinear Proportional Integral Derivative (BPID) controller was employed [30].

B. EMG ACQUISITION, SEGMENTATION AND GESTURE CLASSIFICATION

This section describes the electromyographic information acquisition system and their processing which allows to recognize gestures exerted by a user's hand through the machine learning classifier.

In this work, the commercial Myo Armband sensor, manufactured by the Canadian company Thalmic Labs [32] is used but the proposed algorithm can also be applied to other similar electromyography circuits, for example MindRove armband. This sensor was chosen according to the availability in our laboratory, for its performance, ergonomics, simplicity, small size, and lightweight design.

This has a bracelet shape, with 8 electromyographic sensors, from medical-grade stainless steel [33] capturing signals from the forearm muscles activity with a frequency of 200 Hz, 8 bits per sample for each sensor [34]. According to the working frequency of the Myo Armband and the Nyquist principle, only EMG signals with frequencies up to 100 Hz can be acquired, resulting in the loss of information from high-frequency EMG signals. This represent a limitation in the sEMG signal acquisition considering that almost all of the signal power is located between 10 and 250 Hz, with the most frequency power between 20 and 150 Hz. Although low frequencies are the most significant for gesture classification, the algorithm can be tested with a device that permits the capture of high-frequency signals to evaluate if its response improves. The device is equipped with Bluetooth 4.0 enabling sEMG data transmission to the computer. Also, this has a 9 axis inertial sensor (IMU) with a frequency of 50 Hz [35]. However, for this study, only the signals recorded by the eight EMG sensors will be used.

Data acquisition of the sEMG signals from the Myo Armband was performed using Matlab, assisted by the MyoMex software [36]. After acquiring sEMG signals with the MyoMex, frequencies ranging from 10 to 100 Hz in the spectrum were observed. Additionally, there was a lack of frequencies at 50 Hz. This indicates that the sEMG signals are filtered between 10-100 Hz, with the 50 Hz band being removed to eliminate power line noise. Furthermore, it was observed that the signals were normalized between -1 and 1 before their acquisition. Subsequently, the signals were rectified and segmented into non-overlapping fixed-time windows considering the simplicity of the algorithm and reduced computational cost.

Various functions for feature extraction, including Root Mean Square (RMS), Mean Absolute Value (MAV), Variance of the sEMG (VAR), Simple Square Integral (SSI), Willson amplitude (WAMP, in this work 0.01), Slope sign changes (SSC), and Waveform length (WL), have been utilized. These functions are employed to extract relevant features from the sEMG signals. The length of the signal segments (window) was set to 300 ms. According to the segment length (300 ms) and the acquisition frequency (200 Hz), we use 60 samples per time window for feature extraction. This setup is still considered to operate in real-time, as discussed in [37]. The process, from sEMG acquisition to the classification of the gesture, is illustrated in Figure 2 and consists of: the calibration of the Myo Armband (using its software), signal acquisition, filtering (using Myo Mex), rectification, segmentation of the sEMG signals, feature extraction, and gesture classification.

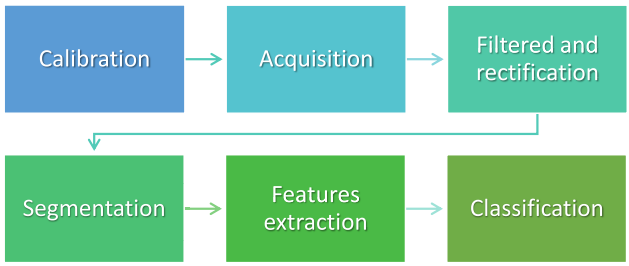

FIGURE 2. Entry process from the data acquisition to the classification.

Given the rectification of the sEMG signal, the ZC feature was omitted from consideration. Additionally, multiple tests were conducted to optimize the feature selection process. To select the combination of the most significant features, classifiers with 5, 4, 3, and 2 input features were built. Each feature was multiplied by 8 sensors, resulting in a total of 40, 32, 24, and 16 inputs, respectively. These classifiers were trained and tested offline using different combinations of features, and the results were analyzed.

C. USER INTERFACE

Six distinct gestures have been proposed for recognition: relax, fit, open hand, pinch, grip, and thumb up, as illustrated in Figure 3. The classification method put forth entails the creation of a personalized dataset for each user, comprising 50 feature samples per gesture (resulting in a total of 300 samples). This dataset personalization is carried out before the initiation of the rehabilitation therapy. It is important to note that the proposed approach involves tailoring the dataset to each individual user and does not rely on a dataset containing samples from different subjects. While this approach enhances the accuracy of gesture recognition, it does require additional time for data acquisition and classifier retraining.

To streamline this process, an automated interface has been developed, as depicted in Figure 4. The figure's bottom portion outlines the sequence of essential steps:

1) Begin by placing the Myo Armband over the forearm and performing the default calibration. In the anatomical position, the armband is positioned on the thick part

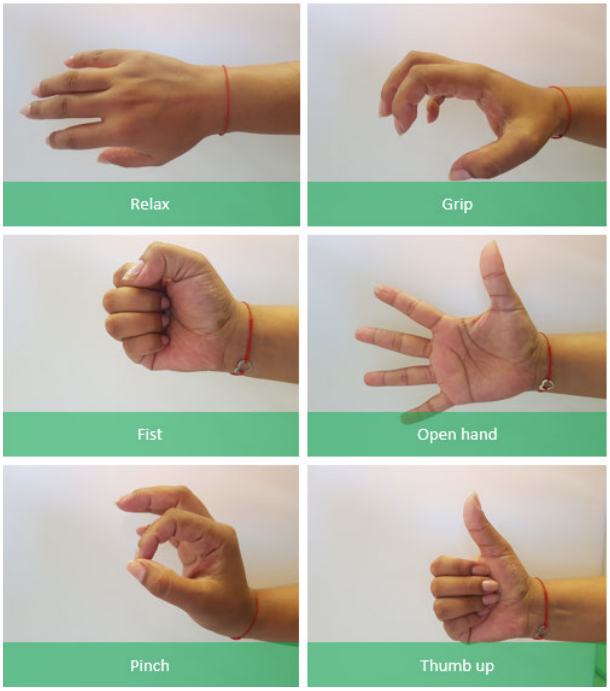

FIGURE 3. Proposed gestures for recognition.

of the forearm, approximately 5 cm above the elbow, with the logo over the center of the extensor muscles and the line sign pointing towards the hand. The default calibration process involves using the Myo Armband application, which prompts the user to perform a 'wave up' gesture (hand extension).

2) After the calibration process, the user is prompted to replicate the target gestures, starting with the relax gesture and concluding with the thumb up gesture.
3) During this process, each gesture is selected one by one (via the buttons outlined in the red dotted line in Figure 4), and 50 samples of each gesture (50 values of the features for each gesture) are recorded and added to the dataset.
4) Once the dataset is complete with all six gestures (resulting in 300 samples), the central button (outlined in the blue dotted line in Figure 4) allows for classifier training.
5) The script automatically organizes all the samples and target data, generating a structured dataset suitable for the Matlab, learning algorithm.

This approach facilitates personalized gesture recognition, providing better accuracy, albeit at the expense of additional data collection and training time.

All processes, from data acquisition to validation for a new user, can vary in duration, typically taking between 2 to 4 minutes. Following this setup, the user can initiate the gesture recognition validation by activating the switch button (encircled by a purple dotted line in Figure 4). When the switch is turned on, the classifier's response is visually represented by LEDs, initially set to yellow. If a gesture is successfully recognized, the LED color changes to green; if not, it remains red.

The final section outlined by a brown dotted line in Figure 4 comprises buttons for connecting with the soft exo-glove. When the gesture verification is active, the first switch labeled "Connect with the Target" can be turned on to establish a connection with the exo-glove system. Subsequently, if the second switch is set to "on," the rehabilitation therapy commences, tailored to the recognized gesture.

D. PROPOSED CLASSIFIERS

Different architectures of classification have been proposed and evaluated: feed forward artificial neural networks (ANN) with one and two hidden layers, K-Nearest-Neighbor (KNN), SVM and Kernel Naive Bayes Classifier. In the training process, the data was divided into 70% for training, 15% for validation, and another 15% for testing, utilizing a five-fold cross-validation. Different ANN architectures with one hidden layer have been tested. The architecture has 24 inputs representing the sEMG characteristics, a different number of neurons in the hidden layer with tansig activation function and 6 output neurons representing the 6 gestures. The output neurons use the purelin activation function.

Also, ANN with two hidden layers was proposed and evaluated. The proposed architecture in this case was: 24 inputs, tansig activation function on the hidden layers (varying the number of neurons) and 6 output neurons with purelin activation function.

The Kernel Naive Bayes (KNB), SVM and the KNN was proposed and tested in the Classification Learner toolbox of Matlab 2022b using different k-fold Cross-validation from 1 to 20.

Finally, the selected classifier algorithm was tested on the NinaPro DB5 dataset [38]. This choice was made according with the hardware used in this study, Myo Armband sensor. The dataset comprises sEMG data from 10 healthy users, captured by two Myo Armband sensors, totaling 16 channels synchronized with the finger joint angles recorded using the CyberGlove, along with the visual stimuli presented to the patients during signal acquisition. Additionally, the dataset includes the biomimetic data of the subjects, such as weight, age, height, gender, and the arm used to perform the test (left or right). The dataset contains EMG data for three types of exercises: basic movements of the fingers, isometric and isotonic hand configurations, basic wrist movements, and grasping and functional movements. According to the proposed methodology, the same gesture was selected from this dataset to test the algorithm: exercise B1 - Thumb up; exercise B6 - all the fingers flexed together in fist; exercise B8 - adduction of the extended fingers; exercise C1 - large diameter grasp; exercise C14 - prismatic pinch grasp; and the hand rest.

The data of this gesture have been extracted and post-processed: segmented each 300 seconds and the features such MAV, RMS and SSC was extracted, and in parallel the gesture was saved for a post-analysis. The KNN algorithm

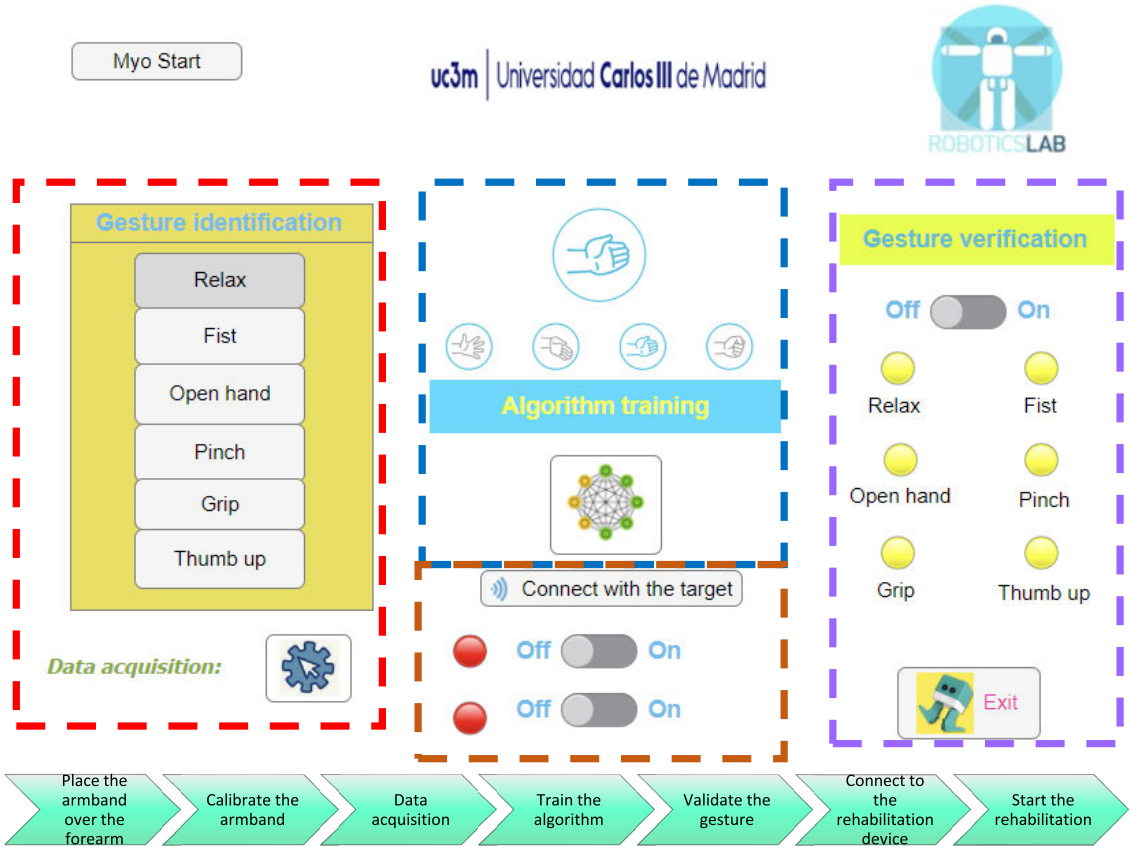

FIGURE 4. Developed interface for gesture recognition and rehabilitation therapy.

was retrained with the extracted features for the sEMG signals for the subjects 1 to 9, splitting the data in training data and test using the five cross validation.

E. HIGH LEVEL CONTROL ALGORITHM

A high-level algorithm was proposed to transition from gesture recognition to actuator control. This algorithm takes the recognized gesture as input and converts it into a position vector. This vector represents maximum displacement values for each finger's actuators and an enable control. For example, when performing a fist gesture, a 7×1 vector is generated (consisting of an enable control and six flexion actuators), with each value set to 45, indicating a 45 mm displacement for the position sensor. This actuator displacement is then doubled through the tendon displacement mechanism, resulting in a 90 mm tendon movement. In the same time, for the extension actuators during a fist gesture, all values are set to 0 mm (control output will be 0) to prevent the opposition to fingers flexion movement.

The maximum values for the flexion or extension movement (position reference) can be customized based on user-specific characteristics. Also, for other gestures, like gripping, the maximum value is configured at 20 mm, and when amplified by the mechanism, it leads to a 40 mm tendon displacement and so on.

Two particular cases are represented by the open hand gesture, which is activated when the first vector position is 1, and the rest of the vector's elements are 0, and the relax gesture when all the vector's elements are set to 0. The limits for the extension actuators are set individually within the software.

From this vector and the current actuator positions, which are directly linked to the tendon' positions, a reference is generated using two types of adjustable increments. The first position vector also serves to initialize or stop the entire system, as the microcontroller receives a 7-position vector. For a visual representation of the proposed algorithm, please refer to Figure 5.

The two increments play a crucial role in generating the position reference. Specifically, the larger increment is used to transition the reference signal from the current position to the actuator's current position, ensuring a rapid movement. Meanwhile, the smaller increment is employed to create a smoother reference. This smaller increment comes into play when the reference signal closely aligns with the actuator's position. Its purpose is to enable the actuator to track the reference signal more accurately in accordance with the gesture's performance.

In the software, the reference limits are determined based on both the maximum sensor and actuator displacements,

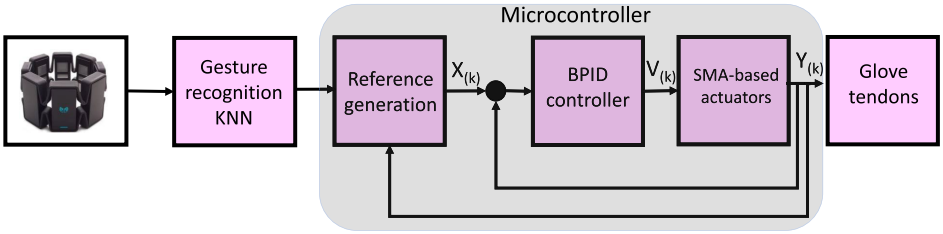

FIGURE 5. High level control algorithm.

as well as the recognized gesture. For instance, in the case of a gripping gesture, the maximum reference can be set at 20 mm.

The soft exo-glove was assessed in an assistive rehabilitation mode using a test bench setup. The Myo Armband was positioned on the user's forearm, while the soft exo-glove was placed to a 3D printed prosthetic hand developed by [39]. Following the calibration of the gesture recognition algorithm, the soft exo-glove was activated via the user interface. Several gestures were tested, and data on the generated reference and tendon positions were recorded.

III. RESULTS

A. FEATURE SELECTION

According to the proposed methodology, models with 5, 4, 3, and 2 input features were tested. A significant decrease in accuracy for models based on 2 input features was observed, while models based on 5, 4, and 3 features showed similar results. Considering computational cost as an important factor, we chose the model based on 3 features. It was observed that features such as SSI, WAMP, VAR, and WL did not yield significant improvements in the classification process. Interestingly, their removal did not result in a decrease in precision, aligning with the findings presented in [40]. The results of the tests, conducted using the proposed classification algorithm with 3 features, are depicted in Figure 6, where the y-axis represents the features that were removed. Based on their contribution to the classification process, we retained the following features: RMS, MAV, and SSC. Considering the eight EMG channels available, this selection results in the extraction of 24 features per segment window: eight RMS, eight MAV and eight SSC.

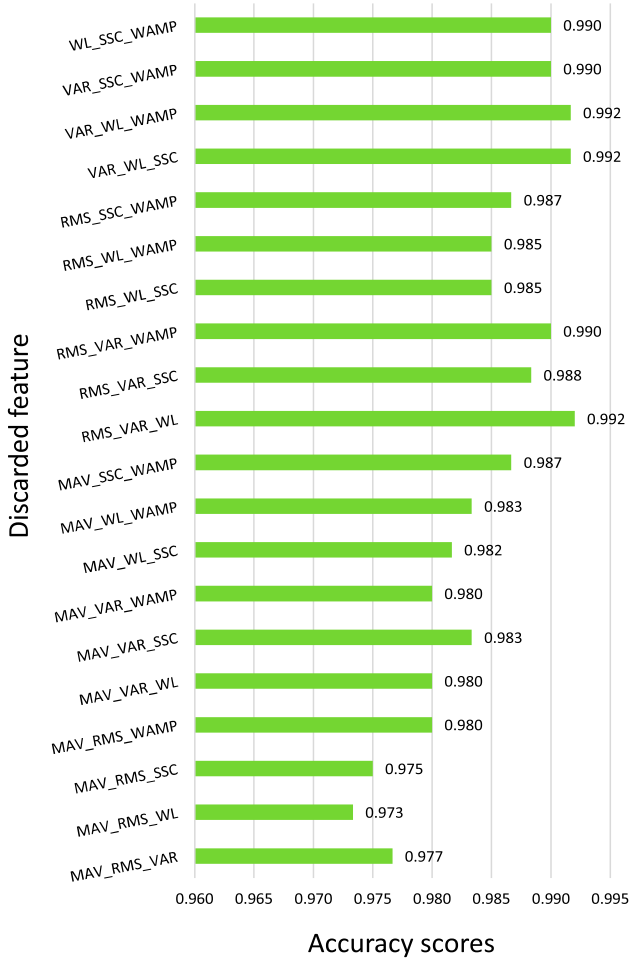

FIGURE 6. Three feature accuracy scores over 1. On the left side, the three discarded features were represented, and on the right side of each bar, the accuracy score over 1 was displayed.

B. CLASSIFIERS PERFORMANCE

The results showed that the ANN with one hidden layer, classifies the gestures well starting from 5 neurons in the hidden layer and the performance of the network not increasing substantially if the number of neurons increment.

On the other hand, the results in the case of a two-hidden-layer ANN demonstrate that the better results start from the configuration with 2 neurons in the first hidden layer and 4 neurons in the second hidden layer.

In the case of KNN and SVM, the better result was obtained with k-fold Cross-validation, $k = 5$. Table 1 presents the most important results of the tested classifiers. As can be seen, all the classifiers have an accuracy superior to 98%. This result was obtained using the test data from the same dataset that was originally divided into training and test sets for classifier training.The better results are obtained with the KNN classifier, both in terms of accuracy and response time. According to these results, although SVM also shows promising results, the KNN classifier was chosen to be used with the soft exo-glove.

TABLE 1. Classifiers results.

Classifier	Better config.	Accuracy	Avg. time for window classification	Max. time for window classification	Avg. response time	Max. response time
KNB	k=5	98.86%	2.60 ms	34.5 ms	20.0 ms	138.0 ms
ANN 1 hidden layer	15 neurons	99.13%	8.40 ms	45.7 ms	33.6 ms	182.8 ms
ANN 2 hidden layers	6 and 10 neurons	99.28%	10.0 ms	22.5 ms	40.0 ms	90.00 ms
KNN	k=5	99.70%	0.25 ms	1.30 ms	20.0 ms	200.0 ms
SVM	k=5	99.35%	0.73 ms	2.30 ms	20.0 ms	200.0 ms

While the proposed method requires approximately 2 to 4 minutes for data acquisition and around 2 seconds for retraining the KNN classifier, it provides commendable accuracy in gesture classification. The classifier can still be utilized even if the bracelet is removed and then replaced, without necessitating the acquisition of a new dataset or retraining. However, it's important to note that the accuracy may diminish under these circumstances.

Furthermore, when transitioning from one user to another without conducting personalized data acquisition, the accuracy may vary. This variation can be attributed to differences in various user characteristics, such as fat levels, hair presence, muscle routing, muscle fatigue, and more.

To assess the classifier's accuracy, several users participated in online testing of the application. Each user was individually prompted to replicate the gestures, and 50 samples of each gesture were recorded, resulting in a total of 300 samples. Subsequently, a personalized KNN classifier was retrained for the first user using their dataset. This user was then asked to repeat the gesture acquisition, and the responses of the KNN classifier were also recorded. Using the KNN output and the desired gestures, a confusion matrix was constructed to evaluate classifier performance.

Figure 7 offers a summary of the KNN classifier's performance in online classification across various users. The specific gestures that experience the most confusion may differ from one user to another. Nevertheless, a common trend is the occurrence of confusion between the pinch and open hand gestures, which can be attributed to the similarity in muscle groups engaged when performing these gestures.

The confusion matrix corresponding to user 10 can be seen in Figure 8, where 15 pinch gestures out of a total of 50 were incorrectly classified as an open hand.

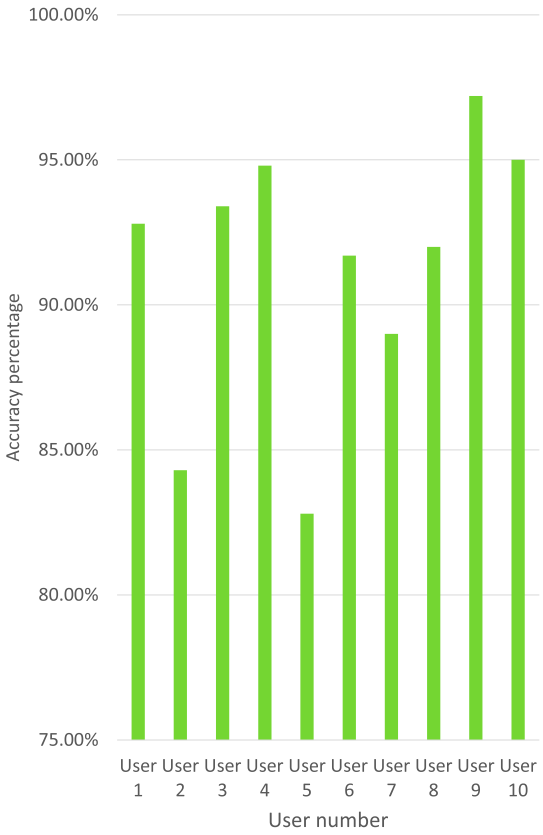

FIGURE 7. Classifiers online results with different users.

C. CLASSIFIER RESULTS OVER NINAPRO DB5

The confusion matrix results, with this dataset can be seen in Figure 9.

According to the confusion matrix presented in Figure 9, the performance of the proposed algorithm shows an 85.2% accuracy. The best identification is associated with Gesture 1 - rest, while the less accurate identifications are observed for the open-hand (Gesture 3) and grip (Gesture 5) gestures.

In addition, Figure 10 depicts the performance of the classifier on the NinaPro DB5 database using the ROC curve. The area under the ROC curve (AUC) represents the integral of the ROC curve (TPR values) with respect to FPR, ranging from FPR $= 0$ to FPR $= 1$. According to Figure 10, all six gestures exhibit good performance, with a minimum AUC of 0.9538 observed for Gesture 3.

Although it is not the primary objective of this work to directly test the trained algorithm with a new user, as the interface recommends data acquisition and algorithm retraining, the algorithm was evaluated with previously unused data from subject 10. In this case, the algorithm achieved an accuracy of 62.6%.

D. PRELIMINARY TEST WITH THE EXO-GLOVE

The final device worn on the human hand can be seen in Figure 11. In this figure, the two sensorized boxes can be observed, along with the activated actuators and the

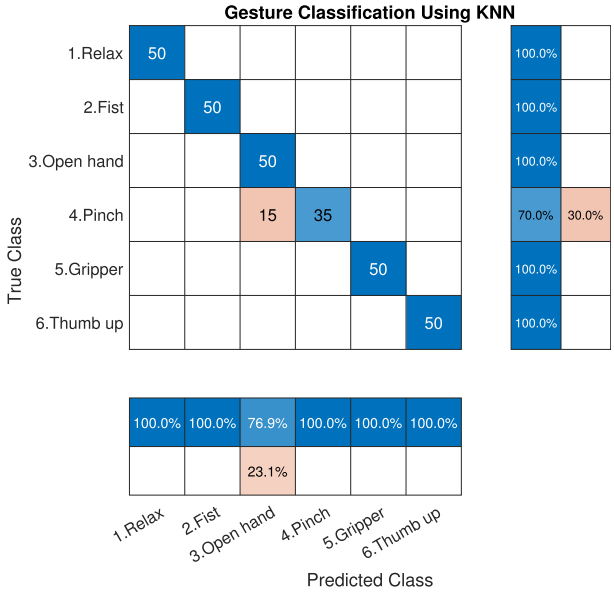

FIGURE 8. Confusion matrix results corresponding to user 10.

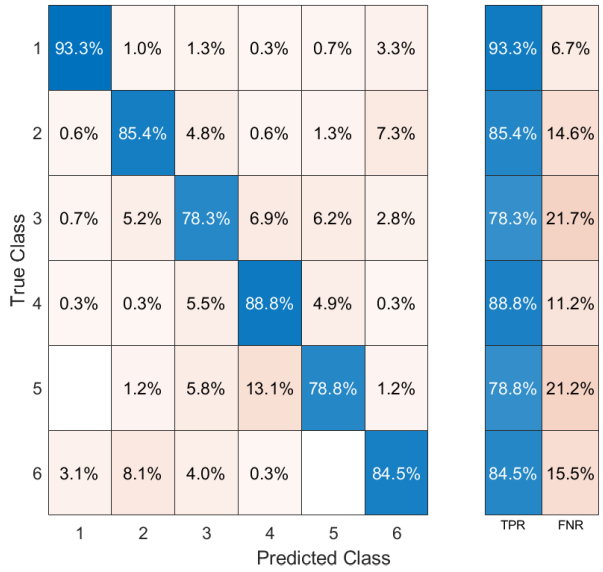

FIGURE 9. Confusion matrix results with the NinaPro DB5.

tense tendons for the fist gesture. Additionally, the wrist is immobilized with the Orliman support.

The proposed soft exo-glove offers three distinct modes of operation:

- Data acquisition mode. Thanks to its flexibility, the soft exo-glove allows for unrestricted movement of the hand and fingers. Simultaneously, sensors gather data on finger movements (glove tendons) and sEMG signals. These data serve both diagnostic purposes for physiotherapists and as a basis for configuring maximum displacement settings for the passive and active rehabilitation modes.
- Passive rehabilitation mode. In this mode, the soft exo-glove adheres to predetermined trajectories, irrespective of the user's intended movements. For instance, each actuator follows a sinusoidal reference pattern.
- Assistive rehabilitation mode. In this mode, the actuators are engaged when the user intends to move, based on gesture recognition. If the user does not express any movement intention, the actuators remain inactive.

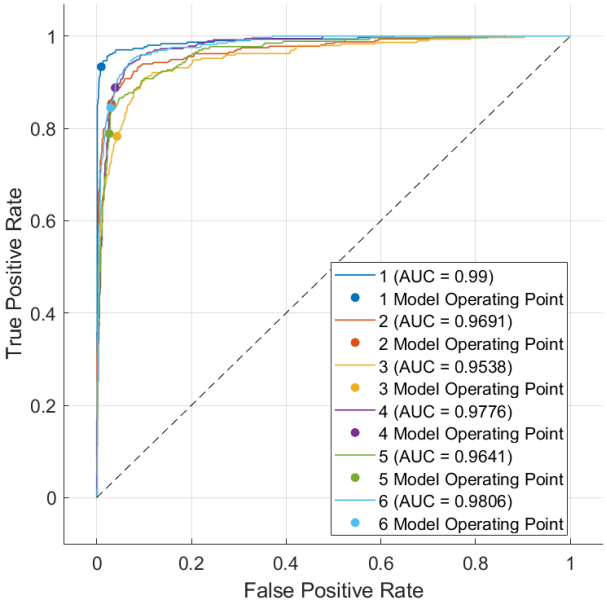

FIGURE 10. ROC curve and the performance metrics with the NinaPro DB5.

The response of the soft exo-glove on the test bench can be observed in Figure 12. In thsi figure, the tendon positions of the five fingers are depicted, following the generated reference based on gesture recognition. Notably, the thumb finger exclusively exhibits the flexion-extension movement, with opposition movement deactivated due to constraints imposed by the prosthetic hand. Depending on the hand's posture, the initial tendon positions differ; for instance, the little finger starts at 22 mm (as shown in Figure 12).

Referring to Figure 12, three gestures were recognized, with relaxation gestures interspersed between them:

- From $t = 0$ to $t = 18$ seconds: Relax gesture.
- From $t = 18$ to $t = 31$ seconds: Fist gesture.
- From $t = 31$ to $t = 60$ seconds: Relax gesture.
- From $t = 60$ to $t = 78$ seconds: Grip gesture.
- From $t = 78$ to $t = 107$ seconds: Relax gesture.
- From $t = 107$ to $t = 122$ seconds: Fist gesture.

The maximum reference value for each finger was determined in accordance with the movement capabilities of the prosthetic hand: 45 mm for the little, middle, and ring fingers, 40 mm for the index finger, and 30 mm for the thumb. Similarly, these maximum reference values can be customized to suit the user's needs.

In Figure 12, it is evident that the generated reference exhibits a steep slope (attributed to a large value increment) until it aligns with the tendon position. Subsequently, a slower reference is generated, which the actuator follows. In this

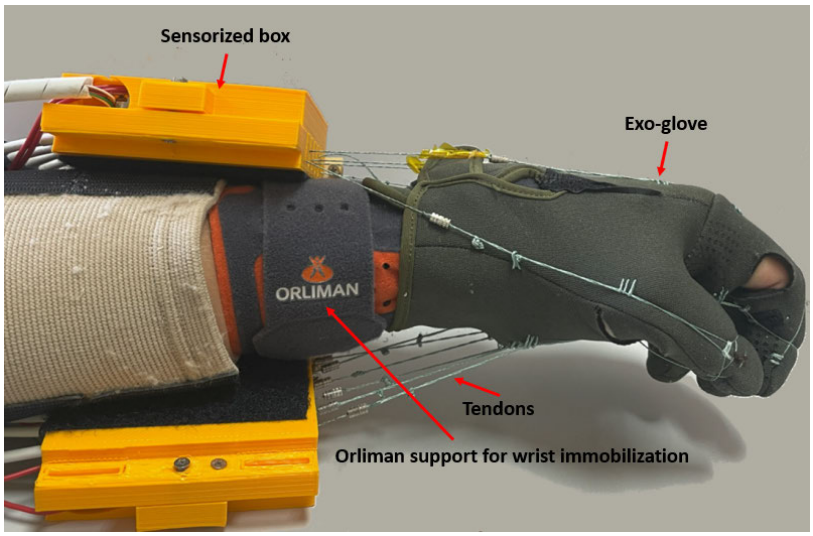

FIGURE 11. Exo-glove worn on the user's hand.

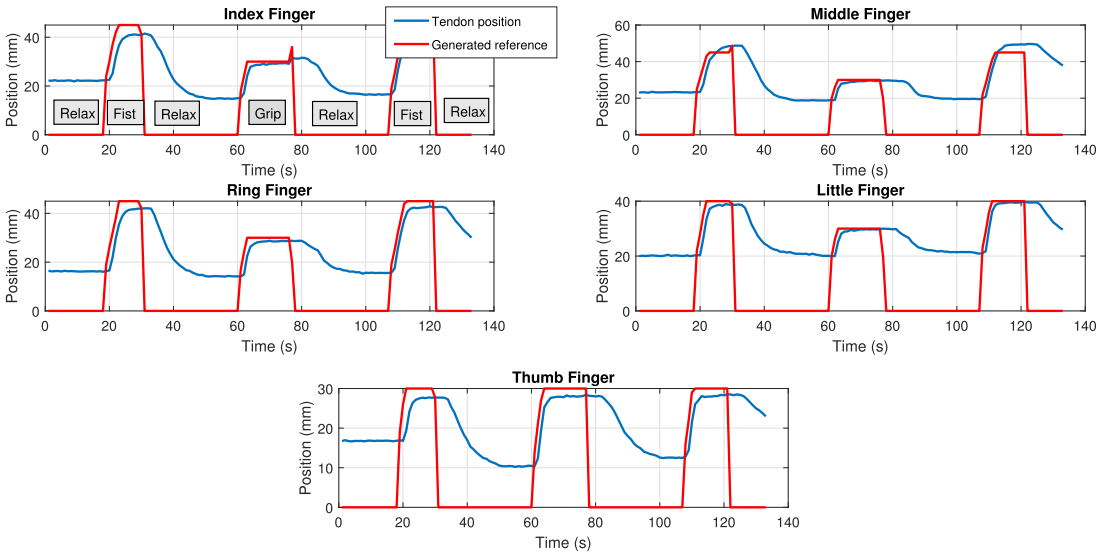

FIGURE 12. Exo-glove position response in the test bench.

scenario, only the flexion actuators are activated to replicate the recognized gesture, as long as the user intends to perform it. The maximum error, which can be minimized by adjusting the BPID gains, is approximately 3 mm.

During finger extension movements, the reference for the flexion actuators is set to 0, indicating that the control signal is at 0, and the actuators are turned off. Meanwhile, the extension actuators can be activated. In such cases, finger movements are constrained by the behavior of the flexion actuators, particularly their thermal characteristics. This constraint can lead to higher errors during extension movements.

The subsequent tests involved placing the proposed device on a human hand and performing fist and pinch gestures. In this scenario, the maximum reference points were determined based on the user's hand dimensions and tendon tension (test error method). For instance, for the fist position, the maximum reference was set to 50 mm for the index, middle, ring, and thumb opposition fingers, and 45 mm for the little and thumb flexion fingers. Figure 13 illustrates the response of the device to the intended movement. Similar to the tests conducted on the test bench, the response of the actuator and tendon position can be observed based on the generated reference.

In both the test bench and when the exo-glove is worn on a human hand, the position error, defined as the difference between the desired reference generated by the high-level algorithm and the actual tendon position, is consistently within a range of 3 mm at its maximum and averages around 2 mm.

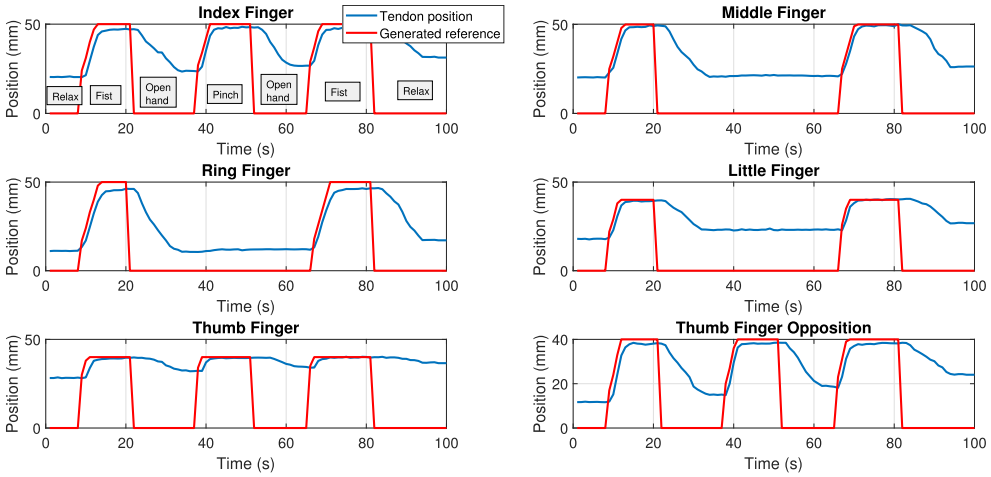

FIGURE 13. Position response of the exo-glove over the user's hand.

IV. DISCUSSION

The comparison of the classifier algorithms with the literature is not appropriate, considering the differences in the EMG detection systems and the number and type of gestures. In this case, informative results can be obtained by considering the results obtained with Nina Pro DB5.

Considering the actuator type, the proposed exo-glove exhibits a limitation when two consecutive movements are antagonistic. For instance, the fist movement, corresponding to the flexion of the fingers, if preceded by an open-hand movement (fingers extension). Due to the thermal actuator behavior, a few seconds are necessary between these two movements to prevent the SMA wires from breaking, leading to the position error increasing, and slowing down the cyclic movements to around 10 seconds which is considered adequate for the rehabilitation tasks [41].

The proposed device features 11 independent actuators, each providing a force of 17.5 N. These actuators enable the independent flexion and extension of the fingers, as well as opposition of the thumb, allowing the device to achieve gestures such as pinch. Thanks to the soft exo-glove structure and the actuator type, the user experiences completely transparent control without any constraints from the device, both when the actuators are not activated and when they are activated based on the user's intended movement. Although the device with this algorithm has not yet been tested with post-stroke patients, which is the next step in this research, it represents a promising, noiseless, and compact soft-glove solution for assistive rehabilitation tasks.

V. CONCLUSION

This contribution introduces a soft exo-glove designed for both passive and assistive rehabilitation tasks, powered by SMA-based actuators. This innovative device empowers users to interact with their environment naturally, free from the constraints of rigid structures. The proposed soft exo-glove is user-friendly, easy to wear like a glove, and offers several advantages, including noiseless operation, a lightweight design, and cost-effective fabrication.

The tendon routing method enables individual finger flexion-extension movements and thumb opposition, utilizing a total of 11 independent actuators (5 for finger extension and 6 for finger flexion) each one with 17.5 N force.

The implemented classifier demonstrates real-time recognition capabilities for commonly used daily-life gestures, achieving an accuracy rate of approximately 90%, with consideration for user-specific variations. Building upon this gesture recognition, an algorithm for generating references for the soft exo-glove was developed and successfully implemented. To streamline the process of gesture recognition and device connectivity for individual users, we have developed a user-friendly interface. This interface facilitates sEMG data acquisition, classifier training, testing, and device connection, enabling the initiation of assistive rehabilitation therapy. To maintain the simplicity of the algorithm and reduce computational costs, a non-overlapping window was chosen. However, in the future, an overlapping window will be implemented, and the results will be compared.

In future endeavors, our focus will center on enhancing the soft exo-glove to make it even more accessible and user-friendly, particularly by improving the existing actuation system. The multi-wire actuator [42] can be implemented to improve the speed of the exo-glove. Additionally, the exo-glove needs to be tested and evaluated with post-stroke patients.

REFERENCES

[1] WH Organization. *Stroke, Cerebrovascular Accident*. Accessed: Oct. 3, 2023. [Online]. Available: https://www.emro.who.int/health-topics/stroke-cerebrovascular-accident/index.html

[2] W. S. Harwin, A. Murgia, and E. K. Stokes, "Assessing the effectiveness of robot facilitated neurorehabilitation for relearning motor skills following a stroke," *Med. Biol. Eng. Comput.*, vol. 49, no. 10, pp. 1093–1102, Oct. 2011.

[3] M.-V. Sánchez-Rebull, A. Terceño Gómez, and Á. Travé Bautista, "Costes de las terapias de las enfermedades neurodegenerativas: Aplicación de un sistema de costes basado en las actividades," *Gaceta Sanitaria*, vol. 27, no. 5, pp. 406–410, Sep. 2013.

[4] F. Zhang, L. Lin, L. Yang, and Y. Fu, "Design of an active and passive control system of hand exoskeleton for rehabilitation," *Appl. Sci.*, vol. 9, no. 11, p. 2291, Jun. 2019.

[5] D. Popov, I. Gaponov, and J.-H. Ryu, "Portable exoskeleton glove with soft structure for hand assistance in activities of daily living," *IEEE/ASME Trans. Mechatronics*, vol. 22, no. 2, pp. 865–875, Apr. 2017.

[6] N. Cheng, K. S. Phua, H. S. Lai, P. K. Tam, K. Y. Tang, K. K. Cheng, R. C. Yeow, K. K. Ang, C. Guan, and J. H. Lim, "Brain–computer interface-based soft robotic glove rehabilitation for stroke," *IEEE Trans. Biomed. Eng.*, vol. 67, no. 12, pp. 3339–3351, Dec. 2020.

[7] Y. Jiang, D. Chen, P. Liu, X. Jiao, Z. Ping, Z. Xu, J. Li, and Y. Xu, "Fishbone-inspired soft robotic glove for hand rehabilitation with multi-degrees-of-freedom," in *Proc. IEEE Int. Conf. Soft Robot. (RoboSoft)*, 2018, pp. 394–399.

[8] X. Chen, L. Gong, L. Wei, S.-C. Yeh, L. Da Xu, L. Zheng, and Z. Zou, "A wearable hand rehabilitation system with soft gloves," *IEEE Trans. Ind. Informat.*, vol. 17, no. 2, pp. 943–952, Feb. 2021.

[9] M. Sierotowicz, N. Lotti, L. Nell, F. Missiroli, R. Alicea, X. Zhang, M. Xiloyannis, R. Rupp, E. Papp, J. Krzywinski, C. Castellini, and L. Masia, "EMG-driven machine learning control of a soft glove for grasping assistance and rehabilitation," *IEEE Robot. Autom. Lett.*, vol. 7, no. 2, pp. 1566–1573, Apr. 2022.

[10] M. Rossi, S. Benatti, E. Farella, and L. Benini, "Hybrid EMG classifier based on HMM and SVM for hand gesture recognition in prosthetics," in *Proc. IEEE Int. Conf. Ind. Technol. (ICIT)*, Mar. 2015, pp. 1700–1705.

[11] M. Tavakoli, C. Benussi, P. Alhais Lopes, L. B. Osorio, and A. T. de Almeida, "Robust hand gesture recognition with a double channel surface EMG wearable armband and SVM classifier," *Biomed. Signal Process. Control*, vol. 46, pp. 121–130, Sep. 2018.

[12] L. Chen, J. Fu, Y. Wu, H. Li, and B. Zheng, "Hand gesture recognition using compact CNN via surface electromyography signals," *Sensors*, vol. 20, no. 3, p. 672, Jan. 2020.

[13] A. R. Asif, A. Waris, S. O. Gilani, M. Jamil, H. Ashraf, M. Shafique, and I. K. Niazi, "Performance evaluation of convolutional neural network for hand gesture recognition using EMG," *Sensors*, vol. 20, no. 6, p. 1642, Mar. 2020.

[14] J. O. Pinzón-Arenas, R. Jiménez-Moreno, and J. E. Herrera-Benavides, "Convolutional neural network for hand gesture recognition using 8 different EMG signals," in *Proc. XXII Symp. Image, Signal Process. Artif. Vis. (STSIVA)*, 2019, pp. 1–5.

[15] X. Chen, Y. Li, R. Hu, X. Zhang, and X. Chen, "Hand gesture recognition based on surface electromyography using convolutional neural network with transfer learning method," *IEEE J. Biomed. Health Informat.*, vol. 25, no. 4, pp. 1292–1304, Apr. 2021.

[16] Y. Cheng, G. Li, M. Yu, D. Jiang, J. Yun, Y. Liu, Y. Liu, and D. Chen, "Gesture recognition based on surface electromyography-feature image," *Concurrency Comput., Pract. Exper.*, vol. 33, no. 6, p. e6051, 2021.

[17] Y. Narayan, "SEMG signal classification using KNN classifier with FD and TFD features," *Mater. Today: Proc.*, vol. 37, pp. 3219–3225, 2021.

[18] A. Devaraj and A. K. Nair, "Hand gesture signal classification using machine learning," in *Proc. Int. Conf. Commun. Signal Process. (ICCSP)*, Jul. 2020, pp. 0390–0394.

[19] Z. Zhang, C. He, and K. Yang, "A novel surface electromyographic signal-based hand gesture prediction using a recurrent neural network," *Sensors*, vol. 20, no. 14, p. 3994, Jul. 2020.

[20] P. Koch, M. Dreier, A. Larsen, T. J. Parbs, M. Maass, H. Phan, and A. Mertins, "Regression of hand movements from sEMG data with recurrent neural networks," in *Proc. 42nd Annu. Int. Conf. IEEE Eng. Med. Biol. Soc. (EMBC)*, 2020, pp. 3783–3787.

[21] T. M. Bittibssi, A. H. Zekry, M. A. Genedy, and S. A. Maged, "SEMG pattern recognition based on recurrent neural network," *Biomed. Signal Process. Control*, vol. 70, Sep. 2021, Art. no. 103048.

[22] W. Song, Q. Han, Z. Lin, N. Yan, D. Luo, Y. Liao, M. Zhang, Z. Wang, X. Xie, A. Wang, Y. Chen, and S. Bai, "Design of a flexible wearable smart sEMG recorder integrated gradient boosting decision tree based hand gesture recognition," *IEEE Trans. Biomed. Circuits Syst.*, vol. 13, no. 6, pp. 1563–1574, Dec. 2019.

[23] N. Secciani, M. Bianchi, E. Meli, Y. Volpe, and A. Ridolfi, "A novel application of a surface ElectroMyoGraphy-based control strategy for a hand exoskeleton system: A single-case study," *Int. J. Adv. Robotic Syst.*, vol. 16, no. 1, pp. 1–13, Jan. 2019.

[24] J. Lv, Y. Yang, L. Niu, X. Sun, L. Wang, W. Lin, H. Rong, and L. Zou, "Prediction of hand grip strength based on surface electromyographic signals," *J. King Saud Univ. Comput. Inf. Sci.*, vol. 35, no. 5, May 2023, Art. no. 101548.

[25] A. Cisnal, P. Gordaliza, J. Pérez Turiel, and J. C. Fraile, "Interaction with a hand rehabilitation exoskeleton in EMG-driven bilateral therapy: Influence of visual biofeedback on the users' performance," *Sensors*, vol. 23, no. 4, p. 2048, Feb. 2023.

[26] L. F. Aguiar and A. P. L. Bo, "Hand gestures recognition using electromyography for bilateral upper limb rehabilitation," in *Proc. IEEE Life Sci. Conf. (LSC)*, Dec. 2017, pp. 63–66.

[27] B. A. De la Cruz-Sánchez, M. Arias-Montiel, and E. Lugo-González, "EMG-controlled hand exoskeleton for assisted bilateral rehabilitation," *Biocybernetics Biomed. Eng.*, vol. 42, no. 2, pp. 596–614, Apr. 2022.

[28] C. Meeker, S. Park, L. Bishop, J. Stein, and M. Ciocarlie, "EMG pattern classification to control a hand orthosis for functional grasp assistance after stroke," in *Proc. IEEE Int. Conf. Rehabil. Robot.*, Feb. 2018, pp. 1203–1210.

[29] Zhang, Yang, Qian, and Zhang, "Real-time surface EMG pattern recognition for hand gestures based on an artificial neural network," *Sensors*, vol. 19, no. 14, p. 3170, Jul. 2019.

[30] D. Serrano, D. Copaci, J. Arias, L. E. Moreno, and D. Blanco, "SMA-based soft exo-glove," *IEEE Robot. Autom. Lett.*, vol. 8, no. 9, pp. 5448–5455, Sep. 2023.

[31] M. Nordin and V. H. Frankel, *Basic Biomechanics of the Musculoskeletal System*. Philadelphia, PA, USA: Lippincott Williams & Wilkins, 2001.

[32] *Thalmic Labs. Medium*. Accessed: Feb. 9, 2021. [Online]. Available: https://medium.com/thalmic

[33] Ö. F. Ertuğrul, S. Dal, Y. Hazar, and E. Aldemir, "Determining relevant features in activity recognition via wearable sensors on the MYO armband," *Arabian J. Sci. Eng.*, vol. 45, no. 12, pp. 10097–10113, Dec. 2020.

[34] Z. Lu, X. Chen, Q. Li, X. Zhang, and P. Zhou, "A hand gesture recognition framework and wearable gesture-based interaction prototype for mobile devices," *IEEE Trans. Hum.-Mach. Syst.*, vol. 44, no. 2, pp. 293–299, Apr. 2014.

[35] M. Vachirapipop, S. Soymat, W. Tiraronnakul, and N. Hnoohom, "Sign translation with myo armbands," in *Proc. 21st Int. Comput. Sci. Eng. Conf. (ICSEC)*, Nov. 2017, pp. 1–5.

[36] M. Tomaszewski. (2017). *Myomex*. Accessed: Feb. 9, 2021. [Online]. Available: https://github.com/mark-toma/MyoMex

[37] J. Valls-Solé, J. C. Rothwell, F. Goulart, G. Cossu, and E. Muñoz, "Patterned ballistic movements triggered by a startle in healthy humans," *J. Physiol.*, vol. 516, no. 3, pp. 931–938, May 1999.

[38] S. Pizzolato, L. Tagliapietra, M. Cognolato, M. Reggiani, H. Müller, and M. Atzori. (2017). *Ninapro Dataset 5 (double Myo Armband) [Data Set]*. Accessed: Jan. 9, 2023. [Online]. Available: https://doi.org/10.5281/zenodo.1000116

[39] *Gyrobot*. Accessed: Jan. 9, 2021. [Online]. Available: http://www.gyrobot.co.uk/

[40] F. Riillo, L. R. Quitadamo, F. Cavrini, E. Gruppioni, C. A. Pinto, N. C. Pastò, L. Sbernini, L. Albero, and G. Saggio, "Optimization of EMG-based hand gesture recognition: Supervised vs. unsupervised data preprocessing on healthy subjects and transradial amputees," *Biomed. Signal Process. Control*, vol. 14, pp. 117–125, Nov. 2014.

[41] J. Lai, A. Song, K. Shi, Q. Ji, Y. Lu, and H. Li, "Design and evaluation of a bidirectional soft glove for hand rehabilitation-assistance tasks," *IEEE Trans. Med. Robot. Bionics*, vol. 5, no. 3, pp. 730–740, Jul. 2023.

[42] J. Arias Guadalupe, D. Copaci, P. Mansilla Navarro, L. Moreno, and D. Blanco, "A novel multi-wire SMA-based actuator with high-frequency displacement," *Mechatronics*, vol. 91, May 2023, Art. no. 102957. [Online]. Available: https://www.sciencedirect.com/science/article/pii/S0957415823000132

DORIN COPACI (Member, IEEE) received the bachelor's degree in automatic control and systems engineering from the Politehnica University of Bucharest, Romania, in 2010, the master's degree in robotics and automation from the Carlos III University of Madrid, Spain, in 2012, and the Ph.D. degree in electrical, electronic, and automatic engineering, in 2017. He is an Assistant Professor with the Department of Systems Engineering and Automation, Carlos III University of Madrid. Since 2010, he has been a Research Member of Robotics Robotics Laboratory. His research primarily focuses on the design and control of emerging actuators and sensors for rehabilitation devices.

DAVID SERRANO DEL CERRO received the bachelor's degree in industrial electronics and automation engineering from Castilla La-Mancha University, in 2016, the master's degree in robotics and automation from the Carlos III University of Madrid, in 2018, and the Ph.D. degree in electrical, electronic and automatic engineering from the System Engineering and Automation Department, Carlos III University of Madrid, in 2023. His research focuses on the design and control of exoskeletons for rehabilitation therapies.

JANETH ARIAS GUADALUPE received the Engineering degree in electronics, control, and industrial networks, in 2011, the master's degree in control systems and industrial automation, and the Ph.D. degree in electrical, electronic, and automatic engineering from the Department of Systems Engineering and Automation, Carlos III University of Madrid. Currently, she is an External Member of Robotics Laboratory, Carlos III University of Madrid, and an Assistant Professor with Universidad Francisco de Vitoria, Madrid. Her professional experience includes research and teaching positions from 2011 to 2018 with Escuela Superior Politécnica de Chimborazo (ESPOCH), Universidad Nacional de Chimborazo (UNACH), Universidad Regional Amazónica IKIAM, and Universidad de las Fuerzas Armadas (ESPE). She has actively participated in various research projects in the fields of rehabilitation robotics and automation.

LUIS MORENO LORENTE (Member, IEEE) received the degree in automation and electronics engineering and the Ph.D. degree from Universidad Politécnica de Madrid, Spain, in 1984 and 1988, respectively. In 1994, he joined the Department of Systems Engineering and Automation, Carlos III University of Madrid, Madrid, Spain, where he has been involved in several mobile robotics projects. His research interests includle mobile robotics, mobile manipulators, environment modeling, path planning, and mobile robot global localization problems.

DOLORES BLANCO ROJAS received the B.S. degree in physics from Universidad Complutense de Madrid, Spain, in 1992, and the Ph.D. degree in mechatronics from the Carlos III University of Madrid (UC3M), in 2002. From 1996 to 1999, she was a Fellowship Student with the Department of Systems Engineering and Automation, UC3M, where she has been an Associate Professor (since 2009) and the Chairperson. She is a member of the Robotics Laboratory Group, UC3M. Her current research interests include sensor based path planning, localization and control for mobile manipulators, and emerging actuator technologies for rehabilitation robotics.